12 Novermber 1999

ELSEVIER

Chemical Physics Letters 313 (1999) 592–599

CHEMICAL PHYSICS LETTERS

www.elsevier.nl/locate/cplett

Density dependent vibrational relaxation in supercritical fluids

D.J. Myers [a], Motoyuki Shigeiwa [a], M.D. Fayer [a,*], Binny J. Cherayil [b]

[a] *Department of Chemistry, Stanford University, Stanford, CA 94305, USA*
[b] *Department of Inorganic and Physical Chemistry, Indian Institute of Science, Bangalore 560034, India*

Received 23 June 1999; in final form 13 September 1999

Abstract

The vibrational lifetimes of the asymmetric CO stretching mode (1990 cm^{-1}) of $W(CO)_6$ in the gas phase and as a function of density in supercritical ethane are examined using infrared pump–probe experiments. The gas phase measurement provides the zero density rate constant, which permits the effect of the ethane solvent to be separated from internal relaxation dynamics. The non-exponential gas phase vibrational dynamics are briefly discussed. The density dependence of the lifetime is compared to an extension of a hydrodynamic theory of vibrational relaxation in supercritical fluids to the regime of large wavevector. Agreement between experiment and theory is found to be good.

1. Introduction

The vibrational lifetime (T_1) of a mode of a polyatomic molecule in a polyatomic solvent is, in part, determined by the interactions of the internal degrees of freedom of the solute with the solvent [1]. If the solvent is a supercritical fluid (SCF), such as ethane, it is possible to examine the role of solute–solvent interactions in vibrational relaxation by changing the solvent density at fixed temperature. Recent T_1 measurements at constant temperature of the asymmetric CO stretching mode of $W(CO)_6$ (1990 cm^{-1}) in several SCFs have shown a steep density dependence at low densities, but at higher densities, a more mild density dependence is observed [2].

There is considerable interest in the nature of solute–solvent interactions in SCFs, and a variety of experimental and theoretical techniques have been brought to bear on the subject [3–7]. One of the fundamental questions involves the role of attractive solute–solvent interactions in SCFs. Solute–solvent attraction that is greater than the solvent–solvent attraction can give rise to enhanced local solvent density (solvent clusters) around a solute, particularly near the critical point [8]. It has been suggested that such local density augmentation can account for anomalous experimental observations of solute properties in SCFs [4,9]. However, in connection with the vibrational relaxation experiments, a theoretical approach was used that was based on the changing solvent properties to account for the density dependence of T_1, and no special solute–solvent interactions were included [10]. The theory was based on an analysis limited to small wavevectors (k), and was only able to describe the experimental data qualita-

* Corresponding author. Fax: +1-650-723-4817; e-mail: fayer@d31mfo.stanford.edu

0009-2614/99/$ - see front matter
PII: S0009-2614(99)01059-3

tively. A scaling argument was used to suggest that very near the critical point, T_1 should be virtually density independent. Again, the scaling argument was based on a small k analysis. Simulations of vibrational relaxation in SCFs, in which the solute–solvent and solvent–solvent interactions are identical, also indicate that no special solute–solvent interactions are necessary to account for the mild density dependence near the critical density [11].

In this Letter, we present new experimental results and theoretical analysis of T_1 for the $W(CO)_6$ asymmetric CO stretching mode in SC ethane. To determine the effect of solvent density on T_1, it is necessary to know T_1 at zero density. At zero density, the vibrational relaxation rate constant $(1/T_1)$ involves relaxation from the initially excited high frequency mode into the large density of states of low frequency intramolecular modes. Subtracting the zero density rate constant from the rate constants measured at finite densities yields the solvent induced contribution to the vibrational relaxation. Because an accurate value of the rate constant at zero density is important, it was measured directly on gas phase $W(CO)_6$. The zero density T_1 is combined with improved measurements of the density dependence of T_1 in SC ethane to yield the vibrational relaxation rate constant as a function of density at two temperatures, 34°C and 50°C (critical temperature, $T_c = 32$°C).

The results of the density dependent vibrational rate constant measurements are compared to a revised version of the previous theory [10]. When the small k approximations were made, it was possible to obtain an analytical expression for the rate constant. In the current work, numerical methods were used to perform the calculations at all k. A form of the hydrodynamic equations is developed that can be used at all k. Evaluation of the resulting expression shows good agreement with the data over a wide range of densities. The theory involves parameters that are obtained from the ethane equation of state. Thus, detailed properties of solvent, including behavior near the critical point, are included in the theory. However, in determining the density dependent spatial distribution of solvent about the solute, the solute and solvent are treated as hard spheres. Thus, no specific solute–solvent attractive interactions are included.

2. Theory

To calculate the solvent contribution to the vibrational relaxation rate in an SCF, it is important to use a method that can incorporate the physical properties of the solvent over a wide range of densities and temperatures. One such method, developed by Cherayil and Fayer [10], is briefly described below. The rate of relaxation from the excited state can be related to the time correlation function of the force, which in turn can be evaluated in terms of known thermodynamic and hydrodynamic properties of the solvent.

The theory starts with the standard relationship between the vibrational lifetime, T_1, and a classical description of the force–force correlation function,

$$k(\rho,T) = T_1^{-1} = \frac{\beta}{m}\int_0^\infty \mathrm{d}t \langle F(t)F(0)\rangle_{\mathrm{cl}} \cos(\omega t). \tag{1}$$

β is $1/k_{\mathrm{B}}T$, where k_{B} is Boltzmann's constant, m is the reduced mass of the oscillator, and ω is the frequency associated with energy deposition into the solvent. The theoretical analysis yields the following expression [10],

$$T_1^{-1} \propto T\int_0^\infty \mathrm{d}t \cos(\omega t)\int \mathrm{d}\boldsymbol{k}\, k^2 |\hat{C}_{21}(\boldsymbol{k})|^2 \hat{S}_1(\boldsymbol{k},t). \tag{2}$$

$\hat{C}_{21}(\boldsymbol{k})$ is the Fourier transform of the direct correlation function between solvent (component 1) and solute (component 2) [12], and $\hat{S}_1(\boldsymbol{k},t)$ is the dynamic structure factor [13].

For small k, $\hat{S}_1(\boldsymbol{k},t)$ can be determined from hydrodynamics as the solution to the coupled equations for the conservation of mass, momentum and energy, which leads to [14]

$$\hat{S}_1(\boldsymbol{k},t) = \hat{S}_1(\boldsymbol{k})\left[\left(1-\frac{1}{\gamma}\right)\mathrm{e}^{-D_T k^2 t} + \frac{1}{\gamma}\cos(c_s k t)\mathrm{e}^{-\Gamma k^2 t}\right] \tag{3}$$

Here $\hat{S}_1(\boldsymbol{k})$ is the equilibrium structure factor of the solvent, which we approximate by the Ornstein–Zernike expression, given by [14]

$$\hat{S}_1(\boldsymbol{k}) = \frac{\rho_1 \kappa_T / \kappa_T^0}{1 + k^2 \xi^2} \tag{4}$$

where ρ_1 is the number density of the solvent, κ_T is its isothermal compressibility, κ_T^0 is the isothermal compressibility of the ideal gas, and ξ is the correlation length of density fluctuations. Further, $\gamma \equiv C_p/C_V$ is the ratio of specific heats, D_T is the thermal diffusivity, c_s is the adiabatic speed of sound, and Γ is the sound attenuation constant. In light scattering experiments, the first term in Eq. (3) corresponds to the zero-frequency Rayleigh peak that is associated with thermal diffusion, while the second term corresponds to twin Brillouin peaks at the frequencies $\pm c_s k$ from the Rayleigh peak that are associated with sound propagation.

Numerical analysis of $\hat{S}_1(\boldsymbol{k},t)$ shows that contributions to the integral in Eq. (2) are overwhelmingly dominated by the function at large k, i.e., $k \approx 1$ Å^{-1} [15]. The first exponential decay time constant in Eq. (3) $1/\tau_1(k)$, ($D_T k^2$ in Eq. (3)) can be extended to large k using an expression by Kawasaki [16]

$$\frac{1}{\tau_1(k)} = \frac{k_B T}{8\pi\eta\xi^3}\left[1 + k^2\xi^2 + \left(k^3\xi^3 - \frac{1}{k\xi}\right)\tan^{-1}(k\xi)\right], \tag{5}$$

where η is the viscosity. For small k, this expression reduces to $D_T k^2$.

There is no general form for the second exponential decay time constant in Eq. (3) $1/\tau_2(k)$, (Γk^2 in Eq. (3)). Since we require $1/\tau_2(k)$ for k corresponding to distances on the order of and smaller than the intermolecular spacing at all densities, we propose an ansatz for its behavior in this region that can be justified with physical arguments, experimental data and theory. In the region of large k, $1/\tau_2(k)$ is assumed to become sufficiently large that the second term on the right hand side of Eq. (3) can be neglected in comparison to the first.

This ansatz is supported by both experiment and theory. For small k, acoustic waves can propagate in the fluid as in a continuum, because the wavelength is much longer than the average intermolecular spacing. In a crystal, the shortest wavelength for a propagating wave is twice the lattice spacing. In a fluid, as the wavelength approaches the average solvent intermolecular spacing, a propagating wave will experience the disorder of the fluid, and such a wave is expected to damp rapidly. For even shorter wavelengths, wave propagation is not possible. These qualitative ideas are born out by neutron scattering experiments [17–19] and molecular dynamics simulations [20,21]. Neutron scattering experiments show that either the Brillouin lines are absent or extremely broad at large k. The broad linewidth is attributed to very rapid damping of large k acoustic waves, i.e., Γ becomes very large. Hard sphere molecular dynamics simulations also show that Γ becomes large at large k and that at sufficiently large k ($k \approx 1.5/$solvent diameter Å^{-1}), acoustic waves do not exist [20]. These considerations support the ansatz that the propagating wave term in Eq. (3) becomes negligible for sufficiently large wavevectors. Therefore, for large k the dynamic structure factor is assumed to be given by,

$$\hat{S}_1(\boldsymbol{k},t) = \hat{S}_1(\boldsymbol{k})\left[\left(1 - \frac{1}{\gamma}\right)e^{-t/\tau_1(k)}\right], \tag{6}$$

with $1/\tau_1(k)$ given by Eq. (5). The equation of state for ethane provides all of the parameters necessary to evaluate Eq. (6).

3. Experimental methods

Infrared vibrational pump–probe experiments were conducted to measure T_1 of the asymmetric stretch of $W(CO)_6$ in both the gas phase and as a function of density in SC ethane. The details of the experiment have been described elsewhere [2,22]. The frequency of the IR OPA is tuned to the peak of the $v = 0 \rightarrow 1$ CO T_{1u} mode absorption of the solute, $W(CO)_6$. The frequency, which depends on the temperature and density of the solvent, is ~ 1990 cm^{-1}.

For experiments conducted in the gas phase, a small amount of solid $W(CO)_6$ was placed in a steel

cell with CaF_2 windows. The cell was evacuated to the point that the vapor pressure of the $W(CO)_6$ was the limiting pressure. The cell was sealed and heated to 50°C to produce enough vapor pressure to conduct the experiment. The pressure is so low that the average collision time is many orders of magnitude longer than the time scale of the measurements. FT-IR spectra of the sample displayed R, Q, and P rotational branches. Experiments discussed here were conducted on the Q branch.

The sample is contained in a high pressure, high temperature cell and sealed with sapphire windows. Two important improvements were made in the SCF sample cell since the previously reported work [2,22–24]. First, a small error in the pressure transducer calibration was corrected. Second, it was found that there was a very small density inhomogeneity in the sample near the critical point. This problem arose from a temperature difference between the sample cell and tubing connecting the cell to pressurizing and measuring equipment. The problem was eliminated by controlling the temperature of the cell and everything connected to it. An enclosure was constructed with heaters and fans to produce a uniform temperature. The sample cell, the valves, the pressure transducer, and connecting tubes were all contained within the enclosure, and all were maintained at the same constant temperature within ± 0.1°C. These improvements did not change any of the previously reported data except those taken very close to the critical point. Full details of the corrected data will be given elsewhere [15].

4. Results and discussion

Fig. 1 shows the extrapolation of six density dependent curves (three solvents, each at two temperatures) to zero density. The spread in the extrapolations comes from making a linear extrapolation using only the lowest density data, which have the largest errors bars. From the extrapolations, the zero density lifetime is ~ 1.1 ns.

All pump–probe measured lifetime decays of $W(CO)_6$ in SC ethane, and in other SCFs such as CO_2 and fluoroform, over a wide range of densities (> 1 mol/l) and temperatures, are single exponentials [2,22,24]. Fig. 2 displays data taken at 326 K on

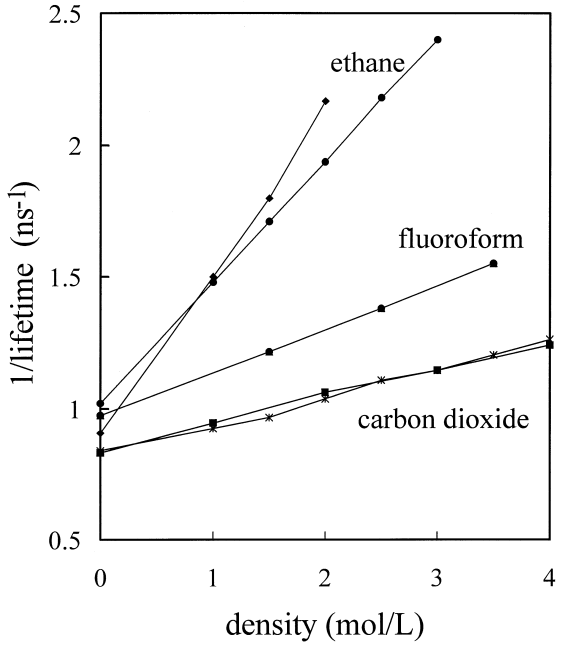

Fig. 1. Extrapolations to zero density of vibrational decay rate constant (1/lifetime) data of the $W(CO)_6$ CO asymmetric stretching mode in supercritical fluids. There are six curves, consisting of two temperatures for three different solvents (ethane, carbon dioxide, and fluoroform). The extrapolations average to a lifetime of ~ 1.1 ns.

the gas phase sample. The data are clearly non-exponential. The data can be fit very well with a tri-exponential. The average values are 140 ps, 1.28 ns, and > 100 ns. These values are well separated in time, permitting reliable separation of the components. The slowest component is too slow to obtain an accurate measurement. The nature of this tri-exponential decay will be discussed in detail elsewhere [25]. Only the qualitative features will be described here.

From the extrapolation to zero density of the density dependent $1/T_1$ data in ethane, fluoroform, and CO_2, as well as experiments in low density Ar [25], it is clear that T_1 is the 1.28 ns decay component. This number is used in the analysis of the density dependent experiments in ethane.

The long component in the decay is caused by 'heating' of the low frequency modes by the relaxation of the ~ 1990 cm^{-1} CO stretch. Since the relaxation occurs without collisions with the solvent,

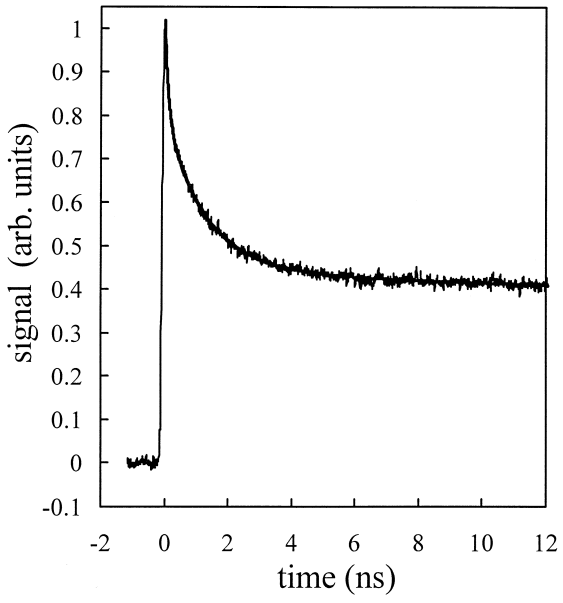

Fig. 2. Infrared pump-probe data for the $W(CO)_6$ CO asymmetric stretching mode in the gas phase at $T = 326$ K. The data are fit with a tri-exponential with decay times of 113 ps, 1.26 ns, and 160 ns. The fit through the data is barely visible. The values given in the text are the average of the fits to a large number of data sets.

the energy remains in the molecule. Calculations using the known frequencies of all of the modes [26] show that depositing $\sim 2000\ cm^{-1}$ into the molecule raises the vibrational temperature from the initial 323 to 450 K. This produces a red shift of the absorption spectrum, which was determined by temperature dependent absorption measurements [25]. The pump–probe signal has two equal parts, ground state depletion and stimulated emission. When the excited CO stretch relaxes into the density of low frequency modes, the contribution to the signal from stimulated emission is lost. This reduces the signal 50%. However, since the spectrum shifts off of the probe pulse wavelength, recovery of the ground state depletion *at the probe wavelength* does not occur. Therefore, the signal decays only 50%. In the absence of collisions that can cool the 'heated' molecules, the signal will remain until collisions occur or cold molecules move into the probed volume. Given the pressure of the sample and the probe spot size (100 μm diameter), the estimated time required for the signal to decay is many ~ 1 μs, which is consistent with the observed very slow decay. When sufficient Ar is added to the cell, the slow decay becomes faster [25], because the Ar can cool the molecules through collisions. At high Ar pressures, the slow component is absent because cooling occurs rapidly compared to the relaxation process. The details of observations on the R, Q, and P branches will be presented in a future publication.

The fastest component (140 ps) will be described theoretically in detail subsequently [25]. We propose that the fast component of the tri-exponential decay (140 ps) can be explained by the influence of the low frequency modes of the molecule on the high frequency CO stretch [25]. In the gas phase vibrational experiment, prior to application of the pump pulse, the initial state of the molecule is prepared by its last collision with the wall of the cell or another molecule. The initial state is a complex superposition of eigenstates. Each mode, λ, will have some occupation number, n_λ. Under collision free conditions, for a given molecule, the n_λ are fixed. At the 326 K sample temperature, the average total internal vibrational energy of a molecule is 2900 cm^{-1}, and the density of states at this energy (calculated with the harmonic approximation) is 5×10^5 states/cm^{-1} [27]. Thus, there are a vast number of initial states of the molecules that comprise the experimental ensemble. Absorbing a photon, which takes a molecule from the 0 to 1 state of the high frequency CO stretch, changes the potential of the low frequency modes. The change in potential produces a time evolution that influences the CO stretch optical transition probability measured by the probe pulse. When a buffer gas or solvent is added, collisions cause the coherent evolution of the slow modes to be interrupted frequently, resulting in a narrowing of the CO asymmetric stretch 0–1 transition and, possibly, an averaging away of the perturbation responsible for the observed fast time dependence. Thus, the fast component observed in these experiments [25] is inherently a low pressure, gas phase phenomenon.

Fig. 3 displays pump–probe data taken in SC ethane at 11 mol/l. The decay is a single exponential as it is at all densities and temperatures studied. The solvent contribution to the rate constant is

$$k(\rho,T) = \frac{1}{T_1^m} - \frac{1}{\boldsymbol{T}_1^g} \qquad (7)$$

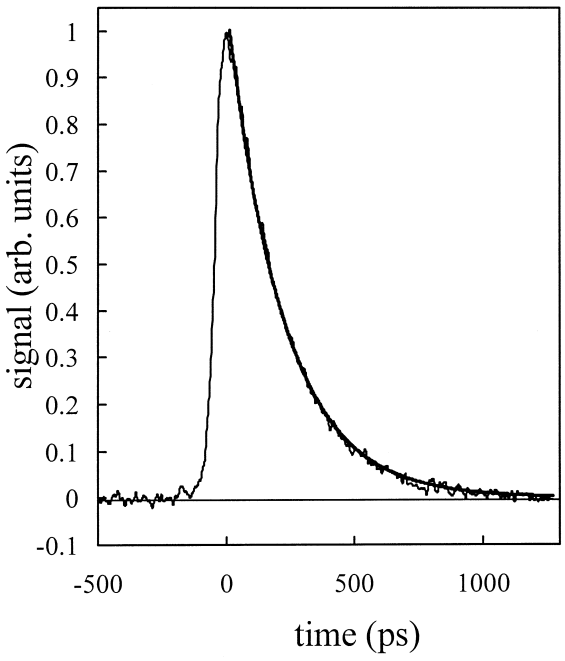

Fig. 3. Infrared pump-probe data for the $W(CO)_6$ CO asymmetric stretching mode in supercritical ethane at 307 K and 11 mol/l. The fit is a single exponential yielding a lifetime of 218 ps. All pump-probe data in ethane are fit well with single exponentials.

where T_1^m is the measure vibrational lifetime at density ρ and temperature T, and T_1^g is the gas phase lifetime, 1.28 ns. Fig. 4 shows the solvent contribution to the vibrational lifetime $(1/k(\rho,T))$ vs. density at two temperatures. The lifetime decreases rapidly as ρ is increased but then becomes flatter at densities greater than ~ 5 mol/l.

The theoretical calculations (solid lines) in Fig. 4 were obtained by evaluating Eq. (2) using Eq. (6). Numerical analysis showed that the contributions to the k integral in Eq. (2) come exclusively from values of k that are sufficiently large that the propagating wave term in Eq. (3) does not come into play. The necessary thermodynamic parameters were obtained from the ethane equation of state [28,29]. A hard sphere model was used for the direct correlation function, $\hat{C}_{21}(\boldsymbol{k})$. $\hat{C}_{21}(\boldsymbol{k})$ describes the spatial distribution of the solvent about the solute. The hard sphere diameter for $W(CO)_6$ (6.70 Å) was calculated from the crystal structure [30]. The hard sphere diameter used for ethane (3.94 Å) is an $\sim 7\%$ reduction of the literature value [31]. Reducing the hard sphere radii by 7% improved the agreement between the theory and the data. The theoretical

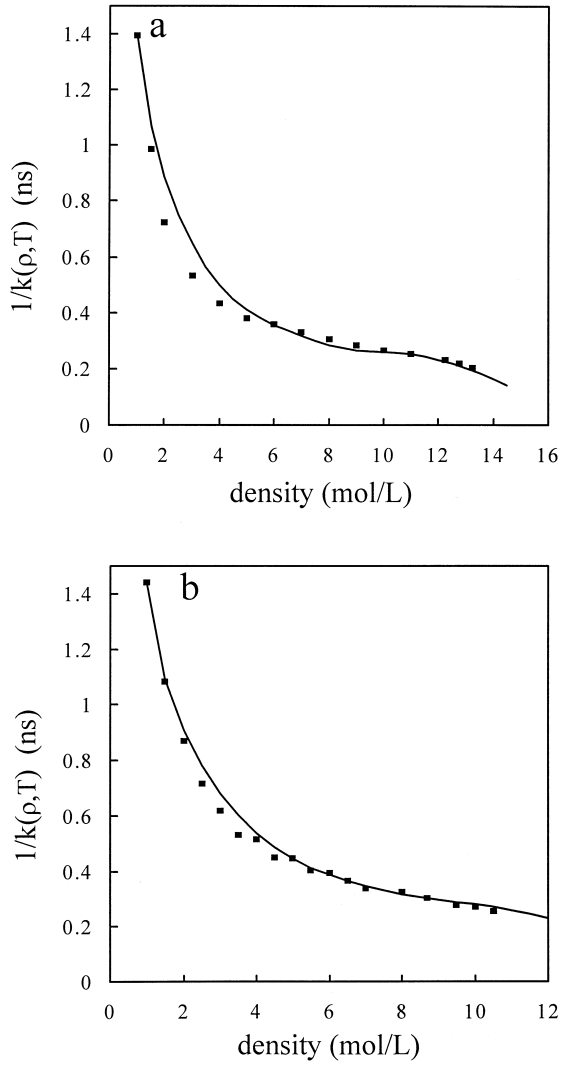

Fig. 4. Experimental solvent contributions to the lifetimes, $1/k(\rho, T)$, (symbols) versus theoretical $1/k(\rho, T)$ (lines) for the $W(CO)_6$ CO asymmetric stretching mode in supercritical ethane as a function of density at two different temperatures. (a) $T = 307$ K. The theory is scaled to the data at the density point 1 mol/l. The Fourier transform frequency, ω, in Eq. (2) is adjusted to obtain the best fit. The ω used in the calculation corresponds to 150 cm^{-1}. The agreement between theory and the data is very good although there is a small systematic deviation. (b) $T = 323$ K. Only the scaling factor at 1 mol/l is adjusted to match the data and theory. The agreement is very good.

curves were scaled to one point (1 mol/l) to account for the absolute strength of the coupling to the solvent and a variety of constants not included in Eq. (2). The scaling does not influence the shape of the calculated curve. The frequency, ω, in the Fourier transform in Eq. (2) is an adjustable parameter that has a significant influence on the shape of the curve. The best agreement was found for an ω corresponding to 150 cm^{-1}. For a diatomic molecule, ω is the vibrational transition energy; relaxation deposits all of the energy into the bath. For the CO asymmetric stretch of $W(CO)_6$, which can undergo vibrational relaxation without participation of a solvent, 150 cm^{-1} is the energy taken up by the bath in the vibrational relaxation process. This energy is almost certainly within the continuum of low frequency modes of the ethane solvent. Instantaneous normal mode calculations in CCl_4, $CHCl_3$, and CS_2 show cut-offs in the DOS at 150, 180, and 200 cm^{-1}, respectively, [32,33]. The higher frequency portions of the DOS are dominated by orientational modes. Since ethane is much lighter than the liquids cited above, it is expected that their DOS will extend to substantially higher frequency. The 150 cm^{-1} may represent a peak in the density of states or the average energy of modes of the solvent participating in the relaxation process.

The fit to the 34°C was obtained by scaling the calculated curve, making the small adjustment in the solvent hard sphere radius and fitting ω. The 50°C calculated curve was obtained with ω and the solvent radius fixed at the values obtained from the 34°C fit. Only the scaling parameter, which does not influence the shape of the curve, was adjusted to obtain the 50°C curve. The agreement between the theory and data is very good. While the data does not change a great deal from 34 to 50°C, most of the thermodynamic input parameters do change significantly. These balance in the theory in a manner that results in a very good description of the data at the two temperatures. The theory has also been applied to data in which fluoroform is the solvent. The equation of state for fluoroform [34] is not as refined as the one for ethane, so there is more uncertainty in the input parameters. The data were compared to theory adjusting only the scaling parameter and a small change in the hard sphere diameter; ω was fixed at 150 cm^{-1}. The agreement is again very good [15]. Comparison between data taken in CO_2 and theory are is not as good as in the other two solvents [15].

The theory uses accurate hydrodynamic and thermodynamic properties of the solvent but a hard sphere description of the direct correlation function. Through the solvent properties, the theory can capture the changing nature of the solvent with density and temperature. There is no specific solute–solvent interaction in the model other than the hard sphere repulsion at contact. Thus it is possible to describe the vibrational relaxation in the solvents studied, without a model that involves an attractive solute–solvent interaction and local density augmentation.

Acknowledgements

We would like to thank the Air Force Office of Scientific Research which made this work possible through grant # F49620-94-1-0141. DJM acknowledges the NSF for a graduate fellowship. MS would like to thank the Mitsubishi Chemical Corporation for supporting his participation in this research.

References

[1] D.W. Oxtoby, Ann. Rev. Phys. Chem. 32 (1981) 77.
[2] R.S. Urdahl, D.J. Myers, K.D. Rector, P.H. Davis, B.J. Cherayil, M.D. Fayer, J. Chem. Phys. 107 (1997) 3747.
[3] D. Schwarzer, J. Troe, M. Zerezke, J. Chem. Phys. 107 (1997) 8380.
[4] Y.-P. Sun, M.A. Fox, K.P. Johnston, J. Am. Chem. Soc. 114 (1992) 1187.
[5] J. Zhang, L.L. Lee, J.F. Brennecke, J. Phys. Chem. 99 (1995) 9268.
[6] I.B. Petsche, P.G. Debenedetti, J. Chem. Phys. 91 (1989) 7075.
[7] D.B. McGuigan, P.A. Monson, Fluid Phase Equilib. 57 (1990) 227.
[8] C.A. Eckert, D.H. Ziger, K.P. Johnston, T.K. Ellison, Fluid Phase Equilib. 14 (1983) 167.
[9] P.G. Debenedetti, S.K. Kumar, AICHE J. 34 (1988) 645.
[10] B.J. Cherayil, M.D. Fayer, J. Chem. Phys. 107 (1997) 7642.
[11] G. Goodyear, S.C. Tucker, J. Chem. Phys. 110 (1999) 3643.
[12] J.L. Lebowitz, Phys. Rev. 133 (1964) 895.
[13] B. Bagchi, J. Chem. Phys. 100 (1994) 6658.
[14] H.E. Stanley, Introduction to Phase Transitions and Critical Phenomena, Oxford, New York, 1971.
[15] D.J. Myers, M. Shigeiwa, M.D. Fayer, B.J. Cherayil, J. Phys. Chem. (1999), submitted for publication.

[16] K. Kawasaki, Ann. Phys. 61 (1970) 1.
[17] T.A. Postol, C.A. Pelizzari, Phys. Rev. A 18 (1978) 2321.
[18] I.M. de Schepper, P. Verkerk, A.A. van Well, L.A. de Graaf, Phys. Rev. Lett. 50 (1983) 974.
[19] U. Bafile, P. Verkerk, F. Barocchi, L.A. de Graaf, J.B. Suck, H. Mutka, Phys. Rev. Lett. 65 (1990) 2394.
[20] W.E. Alley, B.J. Alder, S. Yip, Phys. Rev. A 27 (1983) 3174.
[21] W.E. Alley, B.J. Alder, S. Yip, Phys. Rev. A 27 (1983) 3158.
[22] D.J. Myers, S. Chen, M. Shigeiwa, B.J. Cherayil, M.D. Fayer, J. Chem. Phys. 109 (1998) 5971.
[23] R.S. Urdahl, K.D. Rector, D.J. Myers, P.H. Davis, M.D. Fayer, J. Chem. Phys. 105 (1996) 8973.
[24] D.J. Myers, R.S. Urdahl, B.J. Cherayil, M.D. Fayer, J. Chem. Phys. 107 (1997) 9741.
[25] D.J. Myers, M. Shigeiwa, M.D. Fayer, R.J. Silbey, Chem. Phys. Lett. 312 (1999) 399.
[26] L.H. Jones, R.S. McDowell, M. Goldblatt, Inorg. Chem. 8 (1969) 2349.
[27] D.C. Astholz, J. Troe, W. Wieters, J. Chem. Phys. 70 (1979) 5107.
[28] B.A. Younglove, J.F. Ely, J. Phys. Chem. Ref. Data 16 (1987) 543.
[29] D.G. Friend, H. Ingham, J.F. Ely, J. Phys. Chem. Ref. Data. 20 (1991) 275.
[30] F. Heinemann, H. Schmidt, K. Peters, D. Thiery, Z. Kristallogr. 198 (1992) 123.
[31] D. Ben-Amotz, D.R. Herschbach, J. Phys. Chem. 94 (1990) 1038.
[32] P. Moore, A. Tokmakoff, T. Keyes, M.D. Fayer, J. Chem. Phys. 103 (1995) 3325.
[33] P.B. Moore, X. Ji, H. Ahlborn, B. Space, Chem. Phys. Lett. 296 (1998) 259.
[34] R.G. Rubio, J.A. Zollweg, W.B. Streett, Ber. Bunsenges. Phys. Chem. 93 (1989) 791.